SLAC-PUB-9800
hep-ex/9701013
CLNS 96/1448
CLEO 96-19
January 17, 1997

$\Lambda\overline{\Lambda}$ Production in Two-photon Interactions at CLEO

CLEO Collaboration

Abstract

Using the CLEO detector at the Cornell e^+e^- storage ring, CESR, we study the two-photon production of $\Lambda\overline{\Lambda}$, making the first observation of $\gamma\gamma \to \Lambda\overline{\Lambda}$. We present the cross-section for $\gamma\gamma \to \Lambda\overline{\Lambda}$ as a function of the $\gamma\gamma$ center of mass energy and compare it to that predicted by the quark-diquark model.

Submitted to Physical Review D

Work supported in part by Department of Energy Contract DE-AC03-76SF00515
Stanford Linear Accelerator Center, Stanford University, Stanford, CA 94309, USA

S. Anderson,[1] Y. Kubota,[1] M. Lattery,[1] J. J. O'Neill,[1] S. Patton,[1] R. Poling,[1] T. Riehle,[1] V. Savinov,[1] A. Smith,[1] M. S. Alam,[2] S. B. Athar,[2] Z. Ling,[2] A. H. Mahmood,[2] H. Severini,[2] S. Timm,[2] F. Wappler,[2] A. Anastassov,[3] S. Blinov,[3,1] J. E. Duboscq,[3] D. Fujino,[3,2] R. Fulton,[3] K. K. Gan,[3] T. Hart,[3] K. Honscheid,[3] H. Kagan,[3] R. Kass,[3] J. Lee,[3] M. B. Spencer,[3] M. Sung,[3] A. Undrus,[3,1] R. Wanke,[3] A. Wolf,[3] M. M. Zoeller,[3] B. Nemati,[4] S. J. Richichi,[4] W. R. Ross,[4] P. Skubic,[4] M. Wood,[4] M. Bishai,[5] J. Fast,[5] E. Gerndt,[5] J. W. Hinson,[5] N. Menon,[5] D. H. Miller,[5] E. I. Shibata,[5] I. P. J. Shipsey,[5] M. Yurko,[5] L. Gibbons,[6] S. D. Johnson,[6] Y. Kwon,[6] S. Roberts,[6] E. H. Thorndike,[6] C. P. Jessop,[7] K. Lingel,[7] H. Marsiske,[7] M. L. Perl,[7] S. F. Schaffner,[7] D. Ugolini,[7] R. Wang,[7] X. Zhou,[7] T. E. Coan,[8] V. Fadeyev,[8] I. Korolkov,[8] Y. Maravin,[8] I. Narsky,[8] V. Shelkov,[8] J. Staeck,[8] R. Stroynowski,[8] I. Volobouev,[8] J. Ye,[8] M. Artuso,[9] A. Efimov,[9] F. Frasconi,[9] M. Gao,[9] M. Goldberg,[9] D. He,[9] S. Kopp,[9] G. C. Moneti,[9] R. Mountain,[9] Y. Mukhin,[9] S. Schuh,[9] T. Skwarnicki,[9] S. Stone,[9] G. Viehhauser,[9] X. Xing,[9] J. Bartelt,[10] S. E. Csorna,[10] V. Jain,[10] S. Marka,[10] A. Freyberger,[11] D. Gibaut,[11] R. Godang,[11] K. Kinoshita,[11] I. C. Lai,[11] P. Pomianowski,[11] S. Schrenk,[11] G. Bonvicini,[12] D. Cinabro,[12] R. Greene,[12] L. P. Perera,[12] B. Barish,[13] M. Chadha,[13] S. Chan,[13] G. Eigen,[13] J. S. Miller,[13] C. O'Grady,[13] M. Schmidtler,[13] J. Urheim,[13] A. J. Weinstein,[13] F. Würthwein,[13] D. M. Asner,[14] D. W. Bliss,[14] W. S. Brower,[14] G. Masek,[14] H. P. Paar,[14] M. Sivertz,[14] J. Gronberg,[15] R. Kutschke,[15] D. J. Lange,[15] S. Menary,[15] R. J. Morrison,[15] S. Nakanishi,[15] H. N. Nelson,[15] T. K. Nelson,[15] C. Qiao,[15] J. D. Richman,[15] D. Roberts,[15] A. Ryd,[15] H. Tajima,[15] M. S. Witherell,[15] R. Balest,[16] B. H. Behrens,[16] K. Cho,[16] W. T. Ford,[16] H. Park,[16] P. Rankin,[16] J. Roy,[16] J. G. Smith,[16] J. P. Alexander,[17] C. Bebek,[17] B. E. Berger,[17] K. Berkelman,[17] K. Bloom,[17] D. G. Cassel,[17] H. A. Cho,[17] D. M. Coffman,[17] D. S. Crowcroft,[17] M. Dickson,[17] P. S. Drell,[17] K. M. Ecklund,[17] R. Ehrlich,[17] R. Elia,[17] A. D. Foland,[17] P. Gaidarev,[17] R. S. Galik,[17] B. Gittelman,[17] S. W. Gray,[17] D. L. Hartill,[17] B. K. Heltsley,[17] P. I. Hopman,[17] S. L. Jones,[17] J. Kandaswamy,[17] N. Katayama,[17] P. C. Kim,[17] D. L. Kreinick,[17] T. Lee,[17] Y. Liu,[17] G. S. Ludwig,[17] J. Masui,[17] J. Mevissen,[17] N. B. Mistry,[17] C. R. Ng,[17] E. Nordberg,[17] M. Ogg,[17,3] J. R. Patterson,[17] D. Peterson,[17] D. Riley,[17] A. Soffer,[17] C. Ward,[17] M. Athanas,[18] P. Avery,[18] C. D. Jones,[18] M. Lohner,[18] C. Prescott,[18] S. Yang,[18] J. Yelton,[18] J. Zheng,[18] G. Brandenburg,[19] R. A. Briere,[19] Y.S. Gao,[19] D. Y.-J. Kim,[19] R. Wilson,[19] H. Yamamoto,[19] T. E. Browder,[20] F. Li,[20] Y. Li,[20] J. L. Rodriguez,[20] T. Bergfeld,[21] B. I. Eisenstein,[21] J. Ernst,[21] G. E. Gladding,[21] G. D. Gollin,[21] R. M. Hans,[21] E. Johnson,[21] I. Karliner,[21] M. A. Marsh,[21] M. Palmer,[21] M. Selen,[21] J. J. Thaler,[21] K. W. Edwards,[22] A. Bellerive,[23] R. Janicek,[23] D. B. MacFarlane,[23] K. W. McLean,[23] P. M. Patel,[23] A. J. Sadoff,[24] R. Ammar,[25] P. Baringer,[25] A. Bean,[25] D. Besson,[25] D. Coppage,[25] C. Darling,[25] R. Davis,[25] N. Hancock,[25] S. Kotov,[25] I. Kravchenko,[25] and N. Kwak[25]

[1]University of Minnesota, Minneapolis, Minnesota 55455

---

[1]Permanent address: BINP, RU-630090 Novosibirsk, Russia.

[2]Permanent address: Lawrence Livermore National Laboratory, Livermore, CA 94551.

[3]Permanent address: University of Texas, Austin TX 78712

[2]State University of New York at Albany, Albany, New York 12222
[3]Ohio State University, Columbus, Ohio 43210
[4]University of Oklahoma, Norman, Oklahoma 73019
[5]Purdue University, West Lafayette, Indiana 47907
[6]University of Rochester, Rochester, New York 14627
[7]Stanford Linear Accelerator Center, Stanford University, Stanford, California 94309
[8]Southern Methodist University, Dallas, Texas 75275
[9]Syracuse University, Syracuse, New York 13244
[10]Vanderbilt University, Nashville, Tennessee 37235
[11]Virginia Polytechnic Institute and State University, Blacksburg, Virginia 24061
[12]Wayne State University, Detroit, Michigan 48202
[13]California Institute of Technology, Pasadena, California 91125
[14]University of California, San Diego, La Jolla, California 92093
[15]University of California, Santa Barbara, California 93106
[16]University of Colorado, Boulder, Colorado 80309-0390
[17]Cornell University, Ithaca, New York 14853
[18]University of Florida, Gainesville, Florida 32611
[19]Harvard University, Cambridge, Massachusetts 02138
[20]University of Hawaii at Manoa, Honolulu, Hawaii 96822
[21]University of Illinois, Champaign-Urbana, Illinois 61801
[22]Carleton University and the Institute of Particle Physics, Ottawa, Ontario, Canada K1S 5B6
[23]McGill University and the Institute of Particle Physics, Montréal, Québec, Canada H3A 2T8
[24]Ithaca College, Ithaca, New York 14850
[25]University of Kansas, Lawrence, Kansas 66045

Two-photon interactions are a useful tool for the study of the strong interaction. At CLEO we use two-photon interactions to test calculations of strong processes as well as the understanding of hadron structure. CLEO has previously measured the cross-section for $\gamma\gamma \to p\overline{p}$ [2]. Extending this analysis, in this paper we report on the study of $\gamma\gamma \to \Lambda\overline{\Lambda}$.

Using the Brodsky-Lepage hard-scattering approach [1], predictions have been made for the two-photon production of baryons. The CLEO measurement of the $\gamma\gamma \to p\overline{p}$ cross-section was inconsistent with the prediction of a pure quark model [3] at energies available to CLEO, but was consistent with the prediction of the quark-diquark model [4,5]. We compare the measured $\gamma\gamma \to \Lambda\overline{\Lambda}$ cross-section to that predicted by these models.

CLEO II is a general purpose detector [6] using the e^+e^- storage ring, CESR [7], operating at $\sqrt{s} \sim 10.6$ GeV. CLEO II contains three concentric wire chambers that detect charged particles over 95% of the solid angle. Particle identification is performed using specific ionization energy loss (dE/dx) in the outer wire chamber. A superconducting solenoid provides a magnetic field of 1.5 T, giving a momentum resolution of $\sigma_p/p \approx 0.5\%$ for $p = 1$ GeV. Outside of the wire chambers and a time of flight system, but inside the solenoid, is a CsI electromagnetic calorimeter, consisting of 7800 crystals arranged as two endcaps and a barrel. For a 100 MeV electromagnetic shower in the barrel, the calorimeter achieves an energy resolution of $\sigma_E/E \approx 4\%$.

Kinematics of two-photon events are strongly influenced by the fact that the initial state photons are approximately real and tend to have a large fraction of their momenta along the beam line. A typical $|q^2|$ of the photons is $20\,\mathrm{MeV}^2$, where q is the photon four-momentum. Consequently, the two-photon axis is approximately the beam axis, and the electron and positron rarely have enough transverse momentum to be observed. The two photons have rather unequal energies, causing the $\Lambda\overline{\Lambda}$ center of mass to be boosted along the beam axis. As the available energy in the Λ decay is small, and the $\gamma\gamma \to \Lambda\overline{\Lambda}$ cross-section is peaked near the $\Lambda\overline{\Lambda}$ threshold, the decay products, $p\pi^-\overline{p}\pi^+$, usually have relatively low transverse momentum. We select those events in which all four hadronic tracks are observed in CLEO.

In our analysis of $3.5\,\mathrm{fb}^{-1}$ of data, we use the following selection criteria to minimize background. We select 4 track events in which the charge sum is zero. We require the candidate proton and antiproton to have dE/dx measurements consistent with that of a proton. We require that the event energy, using these particle assignments, is less than 6.0 GeV and that the transverse component of the vector sum of the track momenta is less than 0.6 GeV/c. We veto events in which the candidate Λ or $\overline{\Lambda}$ vertex is at the radius of the beam pipe. We also place a requirement on the transverse impact parameters of the reconstructed Λ and $\overline{\Lambda}$ with respect to the transverse beam position; their root sum square must be less than 1.0 cm. Finally, cross-section predictions [4,8] have been made for $|\cos\theta^*| < 0.6$, where θ^* is the angle between the Λ momentum and the two-photon axis in the two-photon center of mass frame. In order to compare with theory and with $\gamma\gamma \to p\overline{p}$ measurements, we impose the same requirement on the data. As the acceptance of the detector decreases quickly beyond $|\cos\theta^*| = 0.6$, this requirement does not significantly affect the event yield. After applying these selection criteria, there is a clear enhancement in $(m_{p\pi^-}, m_{\overline{p}\pi^+})$ plane at the $(m_\Lambda, m_{\overline{\Lambda}})$ point.

To verify that the reconstructed particles are predominantly Λ's and $\overline{\Lambda}$'s produced in two-photon interactions, a number of data and Monte Carlo distributions have been compared, including event energy, decay distance, Λ momentum angular distribution, proper decay length, acoplanarity, acolinearity, proton momentum, and pion momentum. In all cases there is good agreement between the data and the expected distributions.

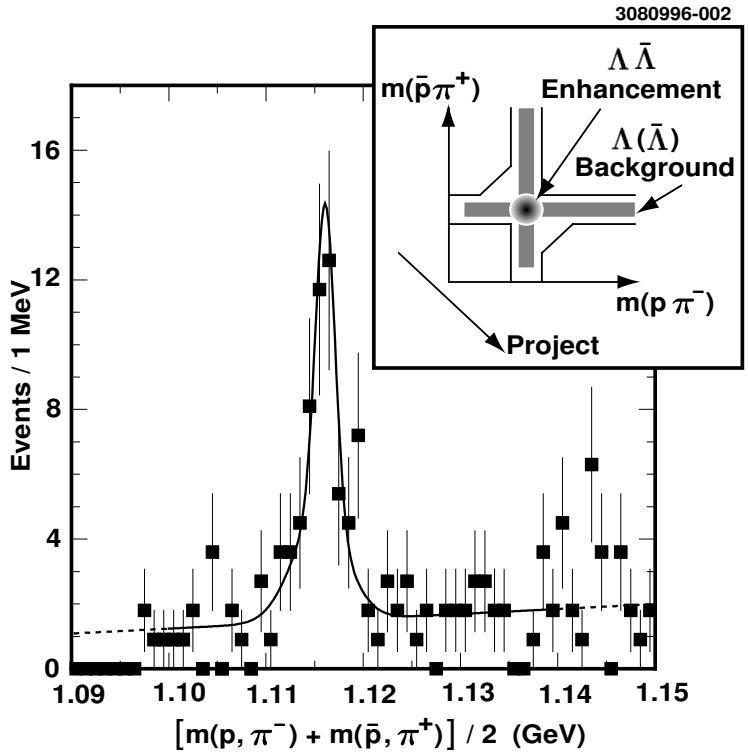

FIG. 1. $\Lambda\overline{\Lambda}$ mass average distribution found in data. Insert depicts mass average projection technique.

The signal and background two-photon Monte Carlo events were generated using a program based on the BGMS formalism [9]. The simulation of the transport and decay of the final state particles through the CLEO detector is performed by a GEANT-based detector simulator [10].

We use the $\Lambda\overline{\Lambda}$ mass average, $(m_{p\pi^-} + m_{\overline{p}\pi^+})/2$, to measure the number of signal events [11]. Viewed geometrically, the mass average rotates the $(m_{p\pi^-}, m_{\overline{p}\pi^+})$ plane by $-\pi/4$ and then scales the projected value by $1/\sqrt{2}$; see Figure 1. The advantage of this approach is that it naturally maps backgrounds from Λ-fake, fake-$\overline{\Lambda}$, and fake-fake into smooth backgrounds in the mass average plot which are then easier to subtract when fitting.

We reduce the fake-fake background by making a geometric selection in the $(m_{p\pi^-}, m_{\overline{p}\pi^+})$ plane before the projection. We require that events are within 6 MeV, nearly 4 times the Λ mass resolution, of the Λ mass for either axis. This simple cross geometry would underestimate fake-fake background near the $\Lambda\overline{\Lambda}$ enhancement. To compensate for this, we extend our geometric criteria at the intersection of the cross so that the area along the projected direction is a constant. This approach is valid as the fake-fake background does not vary significantly near the $\Lambda\overline{\Lambda}$ enhancement.

Using a signal shape fit to the mass average distribution of the Monte Carlo combined with a linear background, we measure 51.0 ± 8.6 events in data. The fit and data are displayed in Figure 1.

Due to reduced sensitivity to other channels and the steep W dependence of two-photon production, the dominant source of feeddown into the observed signal comes from the two-photon production of $\Sigma^o\overline{\Sigma}^o$, $\Lambda\overline{\Sigma}^o$ or $\Sigma^o\overline{\Lambda}$, where W is the two-photon center of mass energy. At this point we have not used final state photon information to distinguish between the four possible final states $(\Lambda/\Sigma^o)(\overline{\Lambda}/\overline{\Sigma}^o)$ for which we use this parenthetical notation to indicate alternative processes.

In order to measure the cross-section we apply the projection technique to the selected data and Monte Carlo events with the addition that we bin in $m_{\Lambda\overline{\Lambda}}$, the effective mass of the Λ and $\overline{\Lambda}$. If the source of the signal is $\gamma\gamma \to \Lambda\overline{\Lambda}$, then $m_{\Lambda\overline{\Lambda}} = W$. We fit to the background excluding the signal region and subtract this from the number of events within the signal region, which is within about 3 times the mass resolution of the Λ mass. The number of events summed over all bins is constrained to be 51.0, the total number of events measured. We have estimated the systematic uncertainty associated with binning, selection criteria, and background shape. The non-negligible sources of uncertainty are associated with triggering, 13%, tracking, 14%, and event selection, 14%. Assuming that these are independent, gives a quadrature sum of 24%, which is conservative in this case.

We find the $e^+e^- \to e^+e^-(\Lambda/\Sigma^o)(\overline{\Lambda}/\overline{\Sigma}^o)$ cross-section in each bin of $m_{\Lambda\overline{\Lambda}}$ by correcting the observed $\Lambda\overline{\Lambda}$ yield in that bin by the efficiency obtained from the Monte Carlo simulation. Summing these we find the total $e^+e^- \to e^+e^-(\Lambda/\Sigma^o)(\overline{\Lambda}/\overline{\Sigma}^o)$ cross-section for $|\cos\theta^*| < 0.6$ to be $2.0 \pm 0.5 \pm 0.5\,\mathrm{pb}$. The first error is statistical, dominated by the statistics of the first bin, the second is the 24% systematic uncertainty discussed above. This corresponds to an overall efficiency of 1.8%.

To correctly extract a cross-section, the contamination from feeddown into the observed signal must be removed. As the statistics are limited, we do not use the mass average technique, but instead we search for either a $(\Sigma^o/\overline{\Sigma}^o)$ in the events that pass all $\Lambda\overline{\Lambda}$ selection criteria described above and that lie within a 6 MeV radius of the point $(m_\Lambda, m_{\overline{\Lambda}})$ in the $(m_{p\pi^-}, m_{\overline{p}\pi^+})$ plane. To search for $(\Sigma^o/\overline{\Sigma}^o)$ we combine each Λ or $\overline{\Lambda}$ with selected photon candidates in the event, using the notation $(\Sigma^o/\overline{\Sigma}^o)$ to indicate either a Σ^o or $\overline{\Sigma}^o$.

We only consider photon candidates in the crystal barrel. The energy associated with the photon candidate must be within the range 40 MeV to 180 MeV. Each candidate photon must not be matched with an observed charged track, and we apply the stricter requirement that the cosine of the angle between the candidate photon and the shower matched with the anti-proton track must be less than 0.9. To reduce background from hadronic interactions, we require that the ratio of energy deposited in the central 9 crystals to that in the central 25 crystals must be > 0.9.

For each $(\Sigma^o/\overline{\Sigma}^o)$ we construct $m_{p\pi\gamma} - m_{p\pi} + m_\Lambda$ which has better resolution than $m_{p\pi\gamma}$. We use a signal shape fit to the Monte Carlo distribution combined with a linear background to fit the data. From the distribution in Figure 2 we measure the number of $(\Sigma^o/\overline{\Sigma}^o)$ to be 7.5 ± 5.6. As the statistical uncertainty associated with this measurement is very large, the systematic uncertainty is not significant. Although consistent with zero, this value will be used to estimate feeddown into the $\gamma\gamma \to \Lambda\overline{\Lambda}$ measurement.

Due to the low statistics of the $(\Sigma^o/\overline{\Sigma}^o)$ measurement, we can not determine the ratio of $\gamma\gamma \to (\Lambda\overline{\Sigma}^o/\Sigma^o\overline{\Lambda})$ to $\gamma\gamma \to \Sigma^o\overline{\Sigma}^o$. We assume that the processes $\gamma\gamma \to (\Lambda\overline{\Sigma}^o/\Sigma^o\overline{\Lambda})$ and $\gamma\gamma \to \Sigma^o\overline{\Sigma}^o$ each contribute half. We assign the difference between the number given by the above mixture of processes and that using the assumption that all observed $(\Sigma^o/\overline{\Sigma}^o)$ events were produced by $\gamma\gamma \to \Sigma^o\overline{\Sigma}^o$ as the systematic uncertainty. Given the above ratio of contributions, we estimate the number of contamination events by multiplying the observed number of $(\Sigma^o/\overline{\Sigma}^o)$ by 4/3 and by the ratio of the $\Lambda\overline{\Lambda}$ detection efficiency to the $(\Sigma^o/\overline{\Sigma}^o)$ detection efficiency in $e^+e^- \to e^+e^-\Sigma^o\overline{\Sigma}^o$ events. We have used the fact that the efficiency for finding a $(\Sigma^o/\overline{\Sigma}^o)$ in $e^+e^- \to e^+e^-\Sigma^o\overline{\Sigma}^o$ events is approximately twice that for finding $(\Sigma^o/\overline{\Sigma}^o)$ in $e^+e^- \to e^+e^-(\Lambda\overline{\Sigma}^o/\Sigma^o\overline{\Lambda})$ events. The estimated number of non-$\Lambda\overline{\Lambda}$ contamination events is $11 \pm 8 \pm 4$, giving a contamination correction scale factor of $[1 - (11 \pm 8 \pm 4)/51.0] = 0.78 \pm 0.16 \pm 0.08$. Applying this factor to the cross-section we extract an exclusive $e^+e^- \to e^+e^-\Lambda\overline{\Lambda}$ cross-section of $1.6 \pm 0.6 \pm 0.4$ pb for $|\cos\theta^*| < 0.6$.

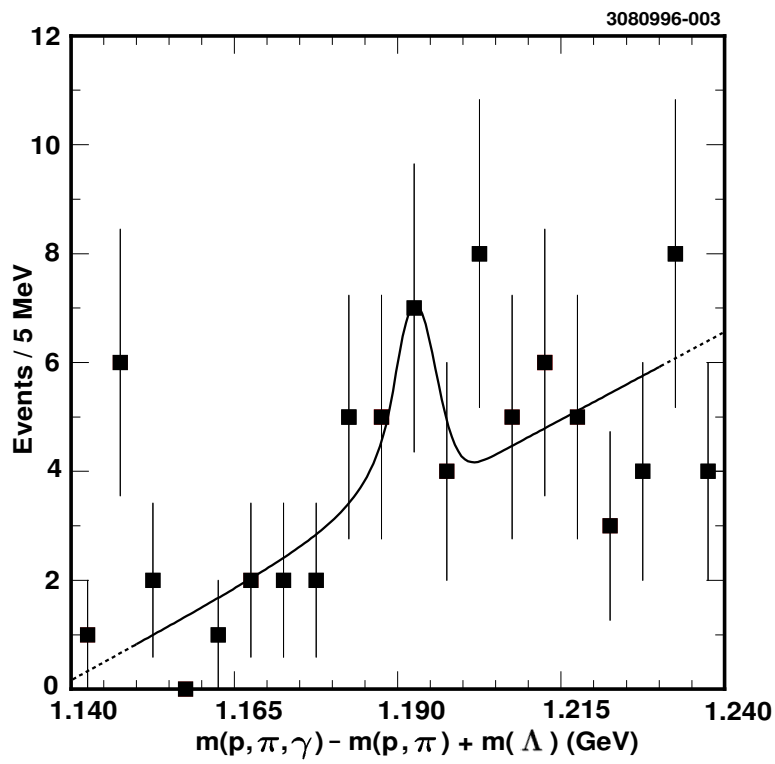

FIG. 2. $(\Sigma^o/\overline{\Sigma}^o)$ mass distribution found in data.

To calculate the $\gamma\gamma \to \Lambda\overline{\Lambda}$ cross-section we scale the measured signal using,

$$\sigma_{bin}^{data} \approx \frac{n_{bin}^{data}/L_{data}}{n_{bin}^{MC}/L_{MC}}\,\sigma_{bin}^{MC}\,, \tag{1}$$

to account for photon flux and efficiency, in each $m_{\Lambda\overline{\Lambda}}$ bin. We correct the cross-section using our estimate of the the $(\Sigma^o/\overline{\Sigma}^o)$ contamination. The $m_{\Lambda\overline{\Lambda}}$ distribution observed in data is a good model for the $m_{\Lambda\overline{\Lambda}}$ distributions of the $\Sigma^o\overline{\Sigma}^o$ and $(\Lambda\overline{\Sigma}^o/\Sigma^o\overline{\Lambda})$ contamination. Consequently, we can apply the contamination correction scale factor bin by bin. The results are shown in Table I. An additional systematic uncertainty associated with the uncertainty of the feeddown $m_{\Lambda\overline{\Lambda}}$ distribution is included.

The predicted $\gamma\gamma \to \Lambda\overline{\Lambda}$ cross-sections appear to disagree with this measurement. Due to the failure of the of pure-quark calculation to accurately predict the cross-section for $\gamma\gamma \to p\overline{p}$ at values of W that we probe, we do not anticipate that it can accurately predict the cross-section for $\gamma\gamma \to \Lambda\overline{\Lambda}$ [3]. However, the quark-diquark model is constructed to predict the cross-section in this energy regime. This model includes nonperturbative effects through the use of the diquark, a qq bound state within the baryon. The original calculations were performed using only scalar diquarks [4]. More recent calculations include both scalar and vector diquarks [5,8]. In the energy regime near threshold, the quark-diquark model is also expected to fail.

The extracted exclusive $\gamma\gamma \to \Lambda\overline{\Lambda}$ cross-section, the previously measured $\gamma\gamma \to p\overline{p}$ cross-section, and the predictions of the model are displayed in Figure 3 as a function of W for $|\cos\theta^*| < 0.6$. We place the horizontal location of the cross-section data points at the weighted mean of W in the bin based on a $\sim 1/W^{12}$ distribution. We do not display the predictions of the pure-quark calculation, which are much smaller than the quark-diquark predictions for both $\gamma\gamma \to p\overline{p}$ and $\gamma\gamma \to \Lambda\overline{\Lambda}$. The

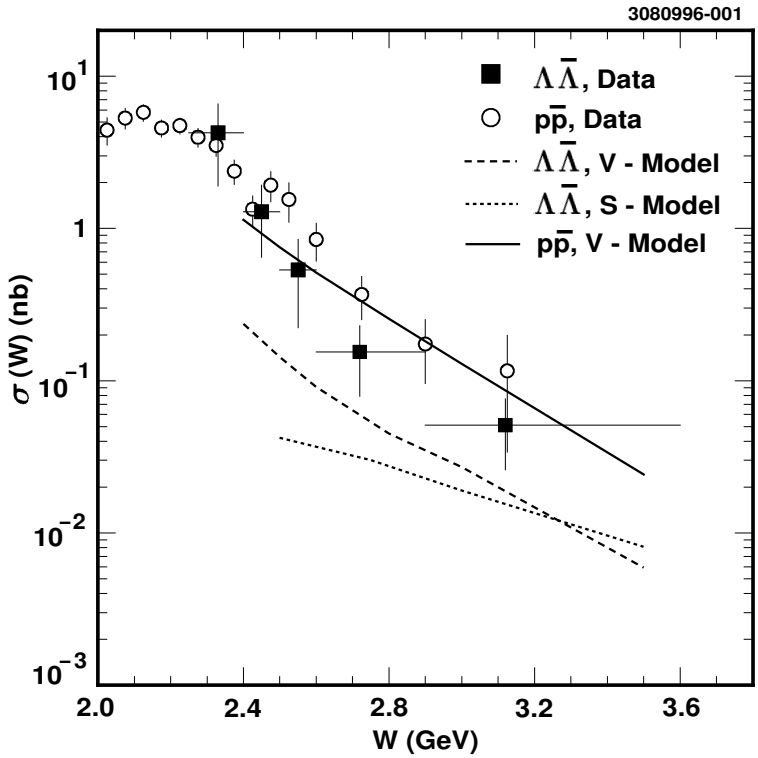

FIG. 3. $\sigma_{\gamma\gamma\to\Lambda\overline{\Lambda}}(W)$, $\sigma_{\gamma\gamma\to p\overline{p}}(W)$ for $|\cos\theta^*| < 0.6$. Vertical error-bars include systematic uncertainties. Horizontal markings indicate bin width. S-model identifies the scalar quark-diquark model [4]. V-model identifies the vector quark-diquark model [5,8].

unexpected result is that the production of $\gamma\gamma \to \Lambda\overline{\Lambda}$ appears to be consistently larger than the prediction of the quark-diquark model. In the three bins above 2.5 GeV the vector quark-diquark model predicts that we should observe ~ 10 events, but in data we observe 32 events.

TABLE I. Two-photon cross-section $\gamma\gamma \to \Lambda\overline{\Lambda}$ for $|\cos\theta^*| < 0.6$

$m_{\Lambda\overline{\Lambda}}$ [GeV]	$\sigma_{\gamma\gamma\to\Lambda\overline{\Lambda}}$ [nb]
$2.25 - 2.4$	$4.2 \pm 1.7 \pm 1.6$
$2.4 - 2.5$	$1.3 \pm 0.5 \pm 0.4$
$2.5 - 2.6$	$0.54 \pm 0.27 \pm 0.16$
$2.6 - 2.9$	$0.15 \pm 0.06 \pm 0.04$
$2.9 - 3.6$	$0.051 \pm 0.019 \pm 0.017$

In this paper we presented the first observation of $\gamma\gamma \to \Lambda\overline{\Lambda}$. We measured the $e^+e^- \to e^+e^-\Lambda\overline{\Lambda}$ cross-section, and the $\gamma\gamma \to \Lambda\overline{\Lambda}$ cross-section as a function of $m_{\Lambda\overline{\Lambda}}$, each for $|\cos\theta^*| < 0.6$. The measured $\gamma\gamma \to \Lambda\overline{\Lambda}$ cross-section appears to be larger than that predicted by either the quark-diquark model or the pure-quark calculation over the observed range of W.

We thank P. Kroll and W. Schweiger for access to their calculations. We gratefully acknowledge the effort of the CESR staff in providing us with excellent luminosity and running conditions. This work was supported by the National Science Foundation, the U.S. Department of Energy,

the Heisenberg Foundation, the Alexander von Humboldt Stiftung, the Natural Sciences and Engineering Research Council of Canada, and the A. P. Sloan Foundation.

REFERENCES

[1] G. P. Lepage and S. J. Brodsky, *Phys. Rev.* **D22** 2157 (1980).

[2] CLEO Collaboration, M. Artuso *et al.*, *Phys. Rev. D* **50**, 5484 (1994).

[3] G. Farrar *et al.*, *Nucl. Phys.* **B259**, 702 (1985); **B263**, 746(E) (1986).

[4] M. Anselmino, F. Caruso, P. Kroll, and W. Schweiger, *Int. J. Modern Phys. A.* **4**, 5213 (1989).

[5] P. Kroll, T. Pilsner, M. Schürmann, and W.Schweiger, *Phys. Lett. B* **316**, 546 (1993).

[6] CLEO Collaboration, Y.Kubota *et al. Nucl. Instr. & Meth.* **A320**, 66 (1992).

[7] D. Rubin, *Proceedings of the 1995 Particle Accelerator Conference* **1**, 481 (1995).

[8] Cross-section including vector diquarks via private communication with P. Kroll and W. Schweiger (1995).

[9] V. M. Budnev, I. F. Ginzburg, G. V. Meledin, and V. G. Serbo, *Phys. Rep.* **15C**, 181 (1975).

[10] R.Brun *et al.*, "GEANT3 Users Guide," CERN DD/EE/84-1 (1987).

[11] H. P. Paar representing the CLEO Collaboration, in *Photon '95, Gamma-Gamma Collisions and Related Processes*, edited by D. J. Miller *et al.*, (World Scientific, 1995).